

Chemically defined generation of human cardiomyocytes

Paul W Burridge^{1–3}, Elena Matsa^{1–3}, Praveen Shukla^{1–3}, Ziliang C Lin⁴, Jared M Churko^{1–3}, Antje D Ebert^{1–3}, Feng Lan^{1–3}, Sebastian Diecke^{1–3}, Bruno Huber^{1–3}, Nicholas M Mordwinkin^{1–3}, Jordan R Plews^{1–3}, Oscar J Abilez^{1–3}, Bianxiao Cui⁵, Joseph D Gold¹ & Joseph C Wu^{1–3}

Existing methods for human induced pluripotent stem cell (hiPSC) cardiac differentiation are efficient but require complex, undefined medium constituents that hinder further elucidation of the molecular mechanisms of cardiomyogenesis. Using hiPSCs derived under chemically defined conditions on synthetic matrices, we systematically developed an optimized cardiac differentiation strategy, using a chemically defined medium consisting of just three components: the basal medium RPMI 1640, L-ascorbic acid 2-phosphate and rice-derived recombinant human albumin. Along with small molecule-based induction of differentiation, this protocol produced contractile sheets of up to 95% TNNT2⁺ cardiomyocytes at a yield of up to 100 cardiomyocytes for every input pluripotent cell and was effective in 11 hiPSC lines tested. This chemically defined platform for cardiac specification of hiPSCs will allow the elucidation of cardiomyocyte macromolecular and metabolic requirements and will provide a minimal system for the study of maturation and subtype specification.

hiPSCs are increasingly used in cardiovascular research, including in disease modeling, cardiotoxicity screening, drug discovery and the study of human cardiac development¹. Furthermore, a major aim of the cardiac differentiation field is to provide cells for cellular therapy¹. Each of these objectives requires large numbers (10⁷–10⁹) of cells to be made in a scalable, cost-effective and reproducible fashion, ideally under chemically defined conditions free of animal-derived products.

Progress in differentiation techniques has yielded multiple methods that produce pure cardiac troponin T-positive (TNNT2⁺) cells with relative ease^{2–6}. Methodological improvements have largely concentrated on mimicking the embryonic developmental signals that control mesoderm induction, activin-Nodal, BMP, Wnt and FGF^{2,3,5,7–10}, and subsequent cardiac specification using inhibition of Wnt⁸, BMP³ and TGFβ^{3,11} pathways. Despite this progress, little is known of the pathways and macromolecules required for *in vitro* cardiac differentiation because of the complexity of proprietary media used, the relatively autonomous nature of *in vitro* cardiac differentiation and the complex secretome involved¹².

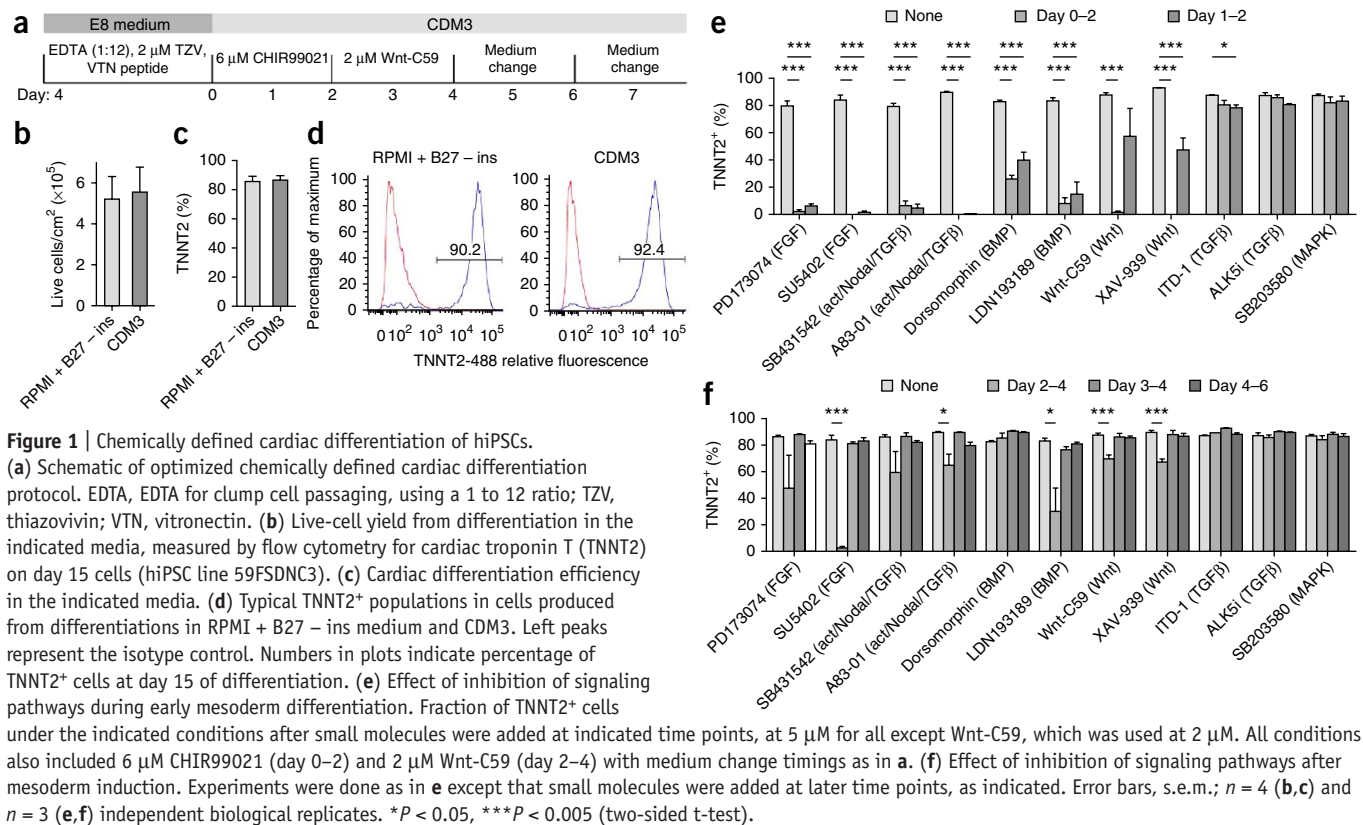
The most efficient protocols to date rely on the basal medium RPMI 1640 (which is chemically defined¹³) supplemented with 'B27', a complex mix of 21 components (many of animal origin), originally designed for the culture of hippocampal neurons¹⁴. It is unknown whether B27 components influence reproducibility of differentiation, maturation or subtype specification. Therefore, we sought to develop an optimized and low-cost cardiac differentiation protocol with no undefined or proprietary medium components, which would enable highly reproducible differentiation and allow further understanding of the macromolecules required for cardiac differentiation. Using our protocol, we reproducibly and efficiently differentiated 11 hiPSC lines (generated under chemically defined conditions) when tested repeatedly from passage 20 to passage 83, which represented >600 differentiations. We produced cardiomyocytes at >85% purity and enriched them to >95% using chemically defined metabolic selection.

RESULTS

A defined cardiac differentiation platform

We generated 11 pluripotent hiPSC lines under chemically defined conditions (**Supplementary Fig. 1**) on a chemically synthesized vitronectin peptide substrate, with nonenzymatic passaging (**Supplementary Fig. 2**). Early experiments had demonstrated that previous monolayer cardiac differentiation protocols⁶ could be adapted to function with hiPSCs grown under chemically defined conditions (**Supplementary Fig. 3**). We concentrated on the three unrelated medium formulations that can support growth factor-based monolayer cardiac differentiation: RPMI medium with B27 supplement without insulin (RPMI + B27 – ins medium)¹⁵, supplemented StemPro-34 medium (ref. 16), and low-insulin albumin polyvinylalcohol essential lipids (LI-APEL) medium⁹ (**Supplementary Table 1**). Initial experiments demonstrated that, of these three, RPMI + B27 – ins medium resulted in the most efficient cardiac differentiation. Starting with the 21 components of B27, we subtracted one component at a time and assessed cultures for continued high-efficiency differentiation (**Supplementary Table 2a–c**). We also assessed components from StemPro-34 and LI-APEL media for potential benefits to differentiation (**Supplementary Table 2d–f**). We concluded that hiPSC

¹Stanford Cardiovascular Institute, Stanford University School of Medicine, Stanford, California, USA. ²Institute for Stem Cell Biology and Regenerative Medicine, Stanford University School of Medicine, Stanford, California, USA. ³Department of Medicine, Division of Cardiology, Stanford University School of Medicine, Stanford, California, USA. ⁴Department of Applied Physics, Stanford University School of Medicine, Stanford, California, USA. ⁵Department of Chemistry, Stanford University School of Medicine, Stanford, California, USA. Correspondence should be addressed to J.C.W. (joewu@stanford.edu) or P.W.B. (burridge@stanford.edu).



cardiac differentiation was successful in a medium consisting of just three components: RPMI 1640 basal medium, L-ascorbic acid 2-phosphate (AA 2-P) and bovine serum albumin (BSA) (Supplementary Table 2g).

Optimization of a chemically defined medium

To render our formula chemically defined and free of animal-derived products, we replaced BSA with recombinant human albumin (rHA; Supplementary Fig. 4a,b). We found that AA 2-P was essential to the formula and observed complete cell death when we omitted it (Supplementary Fig. 4c). Although it was possible to differentiate cells without rHA in an entirely protein-free medium and obtain ~65% TNNT2⁺ cells, the total cell yield was drastically reduced, even when we varied doses of AA 2-P (Supplementary Fig. 4d). Polyvinyl alcohol (PVA), which prevents shear stress in a similar manner to rHA, combined with varying doses of AA 2-P, also did not increase cardiomyocyte yield over that obtained in RPMI 1640 medium with AA 2-P alone. These data suggest that neither prevention of shear stress nor the antioxidant properties of rHA necessitate its inclusion in this formula. We termed our final medium formulation ‘CDM3’ for chemically defined medium, three components; we achieved efficient differentiation with this medium over a broader range (0.8×10^4 to 1.4×10^4 cells/cm²) of initial seeding densities than those for RPMI + B27 – ins medium (1.2×10^4 to 1.4×10^4 cells/cm²; Supplementary Figs. 3d and 4g).

We also assessed six small molecules with GSK3B inhibitory activity to identify whether any of them increased mesoderm induction in CDM3. We observed that only the small molecules BIO and CHIR99021 induced cardiac differentiation; some others were highly toxic (Supplementary Fig. 4h,i). We also assessed small-molecule Wnt inhibitors, many of which were equally effective despite differences

in the inhibition mechanism (Supplementary Fig. 4j,k). Next we analyzed the importance of the timing of canonical Wnt signaling activation with CHIR99021 and Wnt signaling inhibition with Wnt-C59: application of CHIR99021 for 2 d followed by Wnt-C59 for 2 d was optimal in CDM3 but not in RPMI + B27 – ins medium (Supplementary Table 3). The final protocol (Fig. 1a) resulted in production of cardiomyocytes at equivalent yields (Fig. 1b) and efficiencies to those obtained using our optimized protocol with RPMI + B27 – ins medium (Fig. 1c,d). In CDM3, the yield at day 15 was on average 5.5×10^5 TNNT2⁺ cells cm⁻², but as high as 1.25×10^6 TNNT2⁺ cells cm⁻², a 100-fold increase in cell number over the 1.25×10^4 hiPSCs plated at day –4 (4 d before induction of differentiation). We confirmed the specificity of flow cytometry staining conditions for this assay and observed similar percentages of TNNT2⁺ cardiomyocytes using three anti-troponin antibodies (Supplementary Fig. 3g and Online Methods). We observed minimal cell death throughout differentiation (Supplementary Fig. 5), and contraction began at days 7–9 (Supplementary Videos 1–3).

Assessment of essential developmental pathways

We previously proposed that Wnt signaling initiates a paracrine feedback loop via signaling by FGF, BMP, Wnt and activin-Nodal, and may be responsible for mesoderm induction in hiPSCs⁴. To test this hypothesis and to determine whether more specific signaling pathway control could improve robustness of differentiation, we inhibited the six major pathways associated with *in vivo* cardiac differentiation: FGF, activin-Nodal, BMP, Wnt, TGF β and MAPK¹⁷ (Fig. 1e). We added inhibitors of each of these pathways (11 total; Online Methods) at differentiation day 0–2 or day 1–2. Our results demonstrated that FGF, activin-Nodal, BMP and Wnt signaling are essential for mesoderm induction, as inhibition of

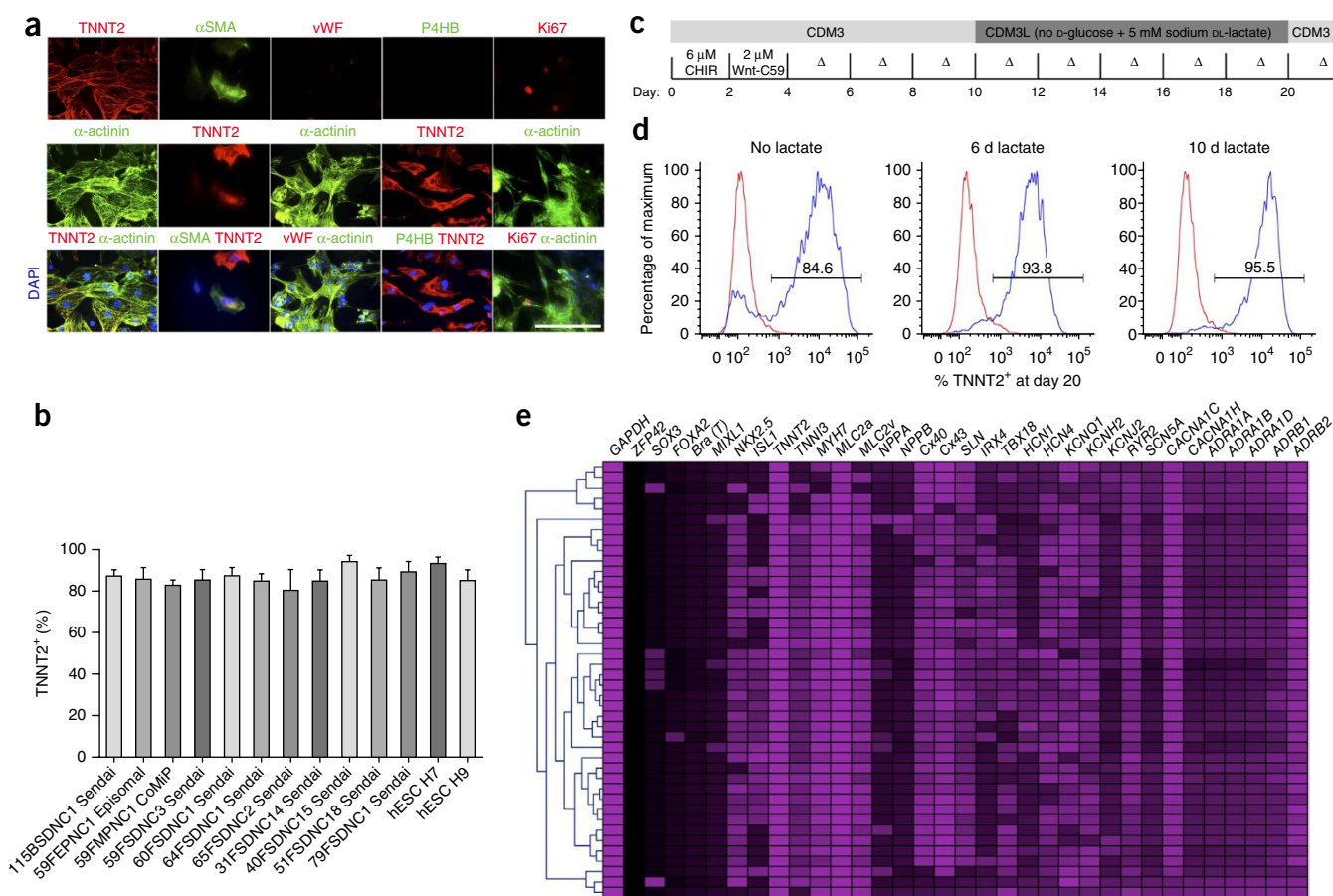


Figure 2 | Characterization and purification of cardiomyocytes produced by chemically defined differentiation. **(a)** Immunofluorescence staining for TNNT2 and α -actinin (cardiomyocyte structural markers), α -smooth muscle actin (α SMA; primitive cardiomyocytes), vWF (endothelial cells), P4HB (fibroblasts) and Ki67 (proliferating cells). Scale bar, 25 μ m. **(b)** Percentage of TNNT2⁺ cells measured by flow cytometry on day 15 of differentiation, in peripheral blood or fibroblast-derived hiPSCs generated with the indicated methods. Dark gray box represents timing of metabolic selection. All hiPSC and hESC lines were cultured under chemically defined conditions and differentiated in CDM3, $n = 3$ –9 independent biological replicates. Error bars, s.e.m. **(c)** Schematic of chemically defined cardiac differentiation including purification by metabolic selection. CDM3L, CDM3 without D-glucose and supplemented with 5 mM sodium D-lactate. Δ , medium change. **(d)** Percentage of TNNT2⁺ cells on day 20 of differentiation, after no treatment, 6 d of treatment (day 10–16) and 10 d treatment (day 10–20). **(e)** Gene expression in single day 20 cardiomyocytes differentiated in CDM3 without metabolic purification, measured by single-cell real-time RT-PCR. Black represents no expression, and light purple represents high expression.

these pathways hindered efficient cardiac differentiation. By contrast, TGF β and p38 MAPK were dispensable (**Fig. 1e**). We then added each of the 11 inhibitors during differentiation days 2–4, 3–4 and 4–6. We found that by days 3–4, none of the six pathways were required because inhibition did not diminish or enhance the efficiency of differentiation (**Fig. 1f**).

CDM3 differentiation on defined matrices

We found that when using the synthetic vitronectin peptide¹⁸ matrix, the highly motile cardiomyocyte monolayers would detach from the surface at ~day 15 (**Supplementary Fig. 6**), irrespective of vitronectin peptide concentrations, which reduced the yield and increased variability. Although this lack of long-term adhesion could be resolved by passaging and replating, we sought a more suitable solution. We first assessed chemically defined pluripotent culture on other defined matrices: recombinant human E-cadherin¹⁹, recombinant human vitronectin²⁰, recombinant human laminin-521 (ref. 21), truncated recombinant human laminin-511 (refs. 22,23), human fibronectin and a fibronectin mimetic (**Supplementary Fig. 7**). The use of

laminin-based matrices resulted in higher growth rates compared to the vitronectin peptide when we correctly optimized surface densities (**Supplementary Fig. 8**), potentially due to the established role of laminin-511 and laminin-521 interacting with $\alpha_6\beta_1$ integrin and activating the PI3K Akt pathway²⁴. Fibronectin-based matrices did not support pluripotent growth. All five suitable matrices supported efficient differentiation in CDM3 (**Supplementary Fig. 6** and **Supplementary Videos 4–9**), and we observed no differences in efficiency between cells cultured long-term (>6 passages) on the defined matrices and cells transferred to the matrix just before differentiation (**Supplementary Fig. 9**). Only the laminin-based matrices maintained long-term adhesion (>15 d) during CDM3 cardiac differentiation (**Supplementary Fig. 6d**), but as these matrices are prohibitively expensive for large-scale application, we performed all subsequent characterization on the vitronectin peptide.

Differentiation in multiple hiPSC lines

Cardiomyocytes produced by CDM3 differentiation were positive for cardiac markers (TNNT2 and α -actinin) and for the immature

cardiomyocyte marker alpha smooth muscle actin (α SMA), and were negative for the endothelial marker von Willebrand factor (vWF) and the fibroblast marker P4HB. A small proportion of cells were positive for the proliferation marker Ki67 (**Fig. 2a**). We tested our protocol with multiple human embryonic stem cell (hESC) and hiPSC lines (Online Methods) at passages between 25 and 80; we observed 80–95% differentiation efficiency for all lines and passage numbers tested, as assessed by flow cytometry for TNNT2 (**Fig. 2b**) as well as yields of greater than 3×10^5 cardiomyocytes cm^{-2} . We could maintain cardiomyocytes in these chemically defined conditions for >200 d.

Enrichment of cardiomyocytes with metabolic selection

Culturing hiPSC-derived cardiomyocytes in glucose-free MEM α supplemented with FBS and lactate has been shown to enrich cells from 4.5% to 98.0% α -actinin-positive²⁵. By replacing the RPMI 1640 medium in CDM3 with RPMI 1640 medium without glucose and supplementing it with sodium DL-lactate (**Fig. 2c**), we found that 6–10 d of glucose deprivation enriched cardiomyocytes from ~85% TNNT2⁺ to >95% TNNT2⁺ (**Fig. 2d**). This method cannot be used in media containing the B27 supplement because it contains a source of glucose (D(+)-galactose). We note that establishing the effects, if any, of metabolic manipulation of cardiomyocytes needs further study.

Characterization of differentiated cardiomyocytes

We sampled the cells differentiating in CDM3 daily and examined gene expression patterns by real-time reverse-transcription (RT)-PCR (**Supplementary Fig. 10**). Consistent with patterns reported for previous differentiation strategies^{2,26} and with embryonic development, the pluripotency marker *POU5F1* was rapidly downregulated at day 2 with concurrent upregulation of the mesoderm markers *T* and *MIXL1*, followed by upregulation of the cardiac mesoderm marker *MESP1*. Early cardiomyocyte markers (*KDR*, *ISL*, and *GATA4*) became highly expressed from days 5–6, with expression of later markers (*NKX2-5*, *TBX5* and *MEF2C*) peaking at days 8–9. Finally, expression of cardiomyocyte myofilament genes *TNNT2* and *MYH6* peaked at days 8–10, and, as previously noted^{2,8}, the expression subsequently decreased, likely owing to the comparatively slow turnover (~3–5 d; ref. 27) of these proteins once the myofilaments were established. Single-cell real-time RT-PCR on day 20 cardiomyocytes (not metabolically selected) showed substantial homogeneity among cells (**Fig. 2e**), although we noted more variation in the expression of the ion channel genes *HCN1*, *HCN4*, *KCNQ1* and *KCNH2*. Many cells coexpressed markers of human atrial (*NPPA*, *CX40* and *SLN*), ventricular (*MLC2V* and *IRX4*)²⁸ and nodal (*TBX18*) cells, which suggested that these day 20 cells are composed of, or still contain, unspecified cardiomyocytes without a fully defined subtype.

To assess the subtypes of cardiomyocytes derived in CDM3, we used flow cytometry to examine cells on days 10, 15, 25, 30, 45 and 60 of differentiation (**Fig. 3a**, and **Supplementary Figs. 11** and **12**). Expression of the two major isoforms of MLC2 (*MLC2A* and *MLC2V*) has been used previously to describe atrial versus ventricular specification of hPSC-derived cardiomyocytes^{5,6,29}. In humans, *MLC2A* expression is detected in both the atria and ventricles during development³⁰ and in adult cardiomyocytes³¹. By contrast, *MLC2V* expression is restricted to the ventricles throughout development and persists into adulthood³⁰. At day 10

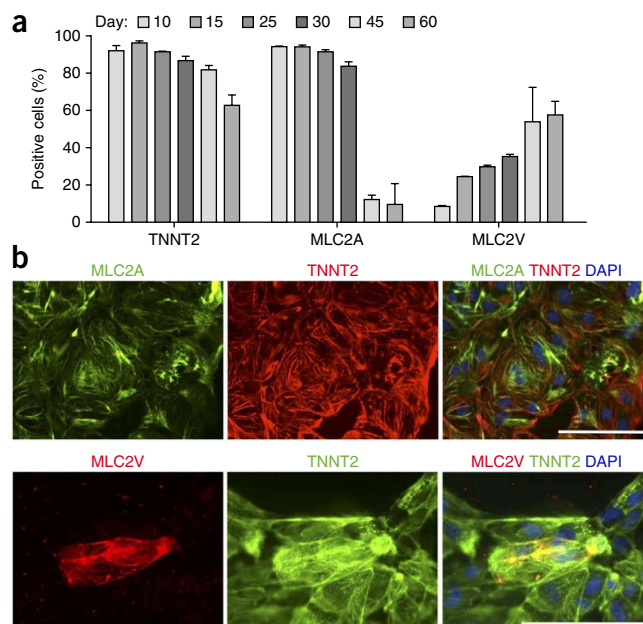


Figure 3 | Characterization of cardiomyocyte subtypes. (a) Flow cytometry analysis of cells positive for TNNT2, MLC2A and MLC2V in cardiomyocytes derived and maintained in CDM3 for the indicated times. $n = 3$ independent biological replicates. Error bars, s.e.m. (b) Immunofluorescence staining of day-20 cardiomyocytes with antibodies to the indicated proteins. Scale bars, 25 μm .

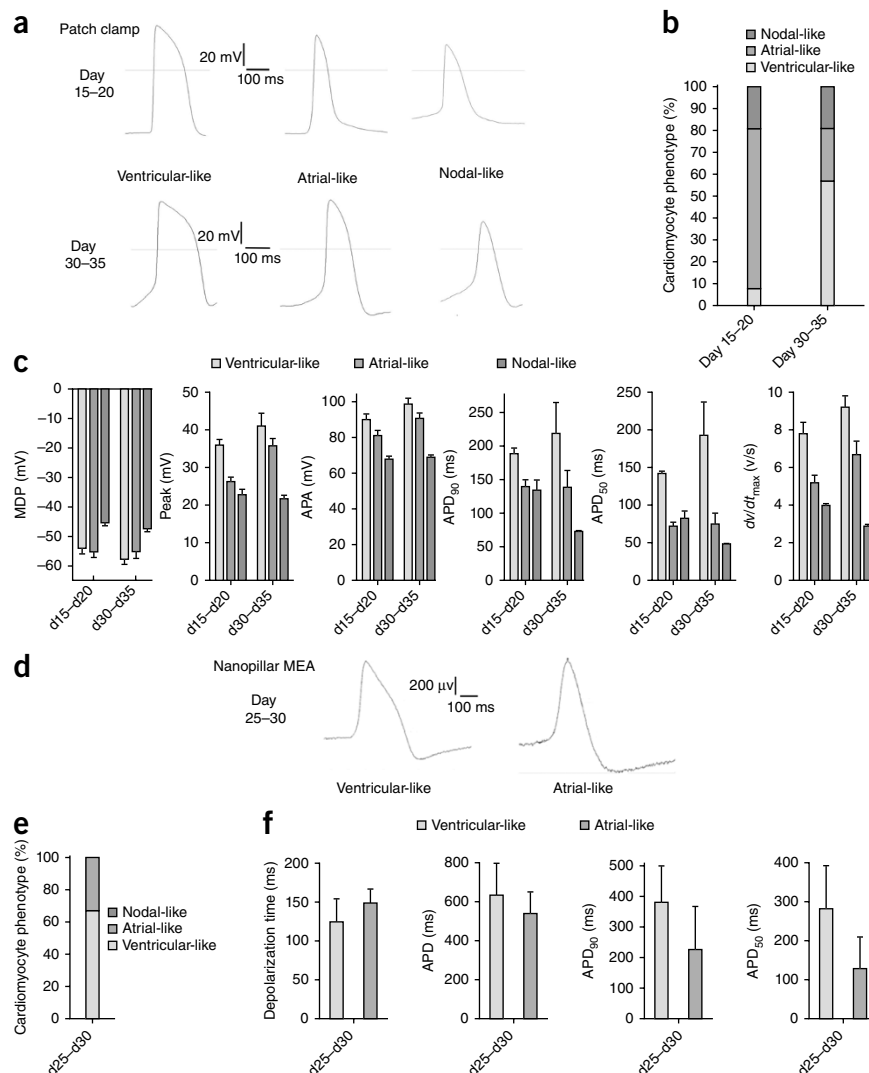
of differentiation, cells demonstrated a TNNT2⁺MLC2A⁺MLC2V⁻ phenotype, likely representing unspecified cardiomyocyte precursors. The number of MLC2A⁺ cells progressively decreased during differentiation, with a dramatic drop to ~10% after day 30, whereas numbers of MLC2V⁺ cells consistently increased, reaching 60% at day 60 (**Fig. 3a**). We confirmed that antibodies labeled sarcomeres by immunofluorescence staining (**Fig. 3b**) and observed similar results in cells differentiated in RPMI + B27 – ins medium (**Supplementary Fig. 11b**).

Patch-clamp analysis demonstrated that at days 15–20, cells had an atrial-like action potential with a low average maximum diastolic potential (MDP) of -55.2 ± 2.0 mV (\pm s.e.m.; **Fig. 4a,b**). These cells likely represented unspecified cardiomyocyte precursors in the heart tube during development and not cells that had undergone atrial specification. At days 30–35, cardiomyocytes demonstrated a more heterogeneous phenotype, with ventricular-like cells being the predominant phenotype (57%, with an MDP of -57.8 mV) along with atrial-like and nodal-like cells (**Fig. 4c** and **Supplementary Table 4**). A second electrophysiological technique, nanopillar electroporation³² confirmed that day 30 cells possessed a predominantly ventricular-like phenotype (**Fig. 4d–f**). Taken together, these electrophysiological analysis data were consistent with our flow cytometry (**Fig. 3a**), immunofluorescence (**Fig. 3b**), and single-cell real-time RT-PCR (**Fig. 2e**) findings, demonstrating that cells differentiated in CDM3 progressed from an unspecified cardiomyocyte precursor phenotype to an immature, predominantly ventricular phenotype.

DISCUSSION

A key surprising finding of our studies was how few medium components are required to differentiate a pluripotent cell to a cardiomyocyte. Of the 21 components in B27, only albumin was required,

Figure 4 | Electrophysiological characterization of cardiomyocytes. (a) Representative action potential recordings using whole-cell patch of three cardiomyocyte subtypes produced from day 15–20 cells ($n = 21$ cells) and day 30–35 cells ($n = 13$ cells). (b) Proportions of cardiomyocyte subtypes at day 15–20 ($n = 21$ cells) and day 30–35 ($n = 13$ cells). (c) Patch clamp recordings of differentiation day (d)15–20 and day 30–35 cells, demonstrating MDP, peak voltage, action potential amplitude (APA), action potential duration (APD) at different levels of repolarization (90% and 50%) and dV/dt_{\max} (maximal rate of depolarization). (d) Action potential traces of ventricular-like and atrial-like subtypes of cells differentiated in CDM3 at day 30 of differentiation and action potential morphology used to classify cardiomyocyte subtype, measured using an MEA-based nanopillar. n values are as above. (e) Percentages of ventricular-like and atrial-like cells measured by nanopillar; $n = 20$ cells. (f) Depolarization time, APD, APD at different levels of repolarization (50% and 90%). Error bars, s.e.m.



and the simple CDM3 medium consisting of three components (recombinant albumin, ascorbic acid and the basal medium RPMI 1640) supported cardiac differentiation at the same efficiency as RPMI + B27 – ins medium.

Albumin can fulfill multiple roles in medium formulations, including acting as a detoxifier or buffer by binding lipids and excessive proteins, binding hormones and growth peptides to keep them stable, and binding free radicals to reduce oxidative damage to cells³³. In CDM3, we used a rice-derived recombinant albumin and can therefore rule out the presence of mammalian albumin-associated proteins, lipids or small molecules. Removal of recombinant albumin from CDM3 did not result in cell death (as with removal of AA 2-P), but merely in a reduction in cardiomyocyte yield. Ascorbic acid is an antioxidant with a well-established role in improving cardiac differentiation^{2,34}, potentially via increasing collagen synthesis that results in greater proliferation of cardiovascular progenitor cells³⁵. The utility of ascorbic acid in E8 medium for pluripotent cell culture and during reprogramming raises the question of whether ascorbic acid is merely acting as an antioxidant in the cardiac differentiation system. Recently, ascorbic acid has been shown to produce widespread but targeted Tet-dependent DNA demethylation³⁶, that may have a role during differentiation. RPMI 1640 medium is one of the simplest classical basal media, related to McCoy's 5A and consisting of 20 amino acids, inorganic salts, the eight B vitamins and the antioxidant glutathione. RPMI 1640 medium does not contain any lipids, iron or zinc, and elucidating the exact reason why this basal medium is superior in this protocol awaits further experimentation.

From repeatedly differentiating 11 hiPSC lines over a range of >60 passages, it became clear that reproducible, highly proliferative

pluripotent growth and prevention of over-confluence was the primary determinant for successful differentiation.

The matrix to which the pluripotent cells are attached is integral in differentiation. In our study, laminin-based matrices were most successful for both the support of pluripotent hiPSC growth and long-term adherence of cardiomyocytes, as seen with human adult cardiomyocytes³¹. It has been demonstrated that hESC-derived cardiomyocytes express integrin α_3 , α_5 , α_6 , α_7 , α_v , β_1 and β_5 (ref. 37), very similar to the predominant expression of α_5 , α_6 , α_v , β_1 and β_5 in pluripotent hESCs²⁰. hESCs adhere to laminin-511, laminin-521 and Matrigel using the $\alpha_6\beta_1$ integrin²², likely explaining the similar long-term adherence performance. By contrast, pluripotent cells adhere to vitronectin using $\alpha_v\beta_5$ integrin^{18,20}, which has a lower binding affinity for its preferred substrates than does $\alpha_6\beta_1$ integrin²³, and along with potential lower expression of $\alpha_v\beta_5$ on hiPSC cardiomyocytes, could explain the differences in long-term cardiomyocyte adherence.

In summary, the chemically defined differentiation medium CDM3 provides a reproducible, scalable method for deriving cardiomyocytes from hiPSCs. Although the cells remain immature, we propose that the chemically simple nature of CDM3, without factors that could skew subtype specification^{38–40}, provides an excellent inert platform to screen for factors to produce

mature atrial, ventricular and nodal cells. Finally, the defined CDM3 medium should help facilitate the translation of basic hiPSC research to the clinic by providing insights into the macromolecular requirements of cardiovascular progenitor cells and hiPSC-derived cardiomyocytes.

METHODS

Methods and any associated references are available in the [online version of the paper](#).

Note: Any Supplementary Information and Source Data files are available in the online version of the paper.

ACKNOWLEDGMENTS

We thank J. Odegaard for analysis of teratoma slides, and K.R. Boheler and R.L. Gundry for their insightful comments on this manuscript. This work was supported by the American Heart Association Postdoctoral Fellowship grant 12POST12050254, Beginning Grant-in-Aid 14BGIA20480329 and US National Institutes of Health K99 HL121177 to P.W.B., and American Heart Association Established Investigator Award 14420025, Foundation Leducq, the National Institutes of Health U01 HL099776, R01 HL113006 and R24 HL117756, and the California Institute for Regenerative Medicine TR3-05556 and DR2-05394 to J.C.W.

AUTHOR CONTRIBUTIONS

P.W.B. conceived, performed and interpreted the experiments and wrote the manuscript; E.M. performed cardiomyocyte immunofluorescence, single-cell RT-PCR and electrophysiology data assessment; P.S., Z.C.L. and O.J.A. performed electrophysiology experiments and assessed data; S.D. provided 'CoMiP' reprogrammed cells; B.H. performed the teratoma assay; J.M.C., A.D.E., F.L., N.M.M. and J.R.P. tested differentiation; B.C. and J.D.G. provided experimental advice; and J.C.W. provided experimental advice, wrote the manuscript and provided funding support.

COMPETING FINANCIAL INTERESTS

The authors declare competing financial interests: details are available in the [online version of the paper](#).

Reprints and permissions information is available online at <http://www.nature.com/reprints/index.html>.

- Matsa, E., Burrridge, P.W. & Wu, J.C. Human stem cells for modeling heart disease and for drug discovery. *Sci. Transl. Med.* **239**, 239ps6 (2014).
- Burrridge, P.W. *et al.* A universal system for highly efficient cardiac differentiation of human induced pluripotent stem cells that eliminates interline variability. *PLoS One* **6**, e18293 (2011).
- Kattman, S.J. *et al.* Stage-specific optimization of activin/nodal and BMP signaling promotes cardiac differentiation of mouse and human pluripotent stem cell lines. *Cell Stem Cell* **8**, 228–240 (2011).
- Burrridge, P.W., Keller, G., Gold, J.D. & Wu, J.C. Production of *de novo* cardiomyocytes: human pluripotent stem cell differentiation and direct reprogramming. *Cell Stem Cell* **10**, 16–28 (2012).
- Zhang, J. *et al.* Extracellular matrix promotes highly efficient cardiac differentiation of human pluripotent stem cells: the matrix sandwich method. *Circ. Res.* **111**, 1125–1136 (2012).
- Lian, X. *et al.* Robust cardiomyocyte differentiation from human pluripotent stem cells via temporal modulation of canonical Wnt signaling. *Proc. Natl. Acad. Sci. USA* **109**, E1848–E1857 (2012).
- Burrridge, P.W. *et al.* Improved human embryonic stem cell embryoid body homogeneity and cardiomyocyte differentiation from a novel V-96 plate aggregation system highlights interline variability. *Stem Cells* **25**, 929–938 (2007).
- Yang, L. *et al.* Human cardiovascular progenitor cells develop from a KDR+ embryonic-stem-cell-derived population. *Nature* **453**, 524–528 (2008).
- Elliott, D.A. *et al.* NKX2-5(eGFP/w) hESCs for isolation of human cardiac progenitors and cardiomyocytes. *Nat. Methods* **8**, 1037–1040 (2011).
- Laflamme, M.A. *et al.* Cardiomyocytes derived from human embryonic stem cells in pro-survival factors enhance function of infarcted rat hearts. *Nat. Biotechnol.* **25**, 1015–1024 (2007).
- Willems, E. *et al.* Small molecule-mediated TGF-beta type II receptor degradation promotes cardiomyogenesis in embryonic stem cells. *Cell Stem Cell* **11**, 242–252 (2012).
- Titmarsh, D.M. *et al.* Microbioreactor arrays for full factorial screening of exogenous and paracrine factors in human embryonic stem cell differentiation. *PLoS One* **7**, e52405 (2012).
- Moore, G.E., Gerner, R.E. & Franklin, H.A. Culture of normal human leukocytes. *J. Am. Med. Assoc.* **199**, 519–524 (1967).
- Brewer, G.J. & Cotman, C.W. Survival and growth of hippocampal neurons in defined medium at low density: advantages of a sandwich culture technique or low oxygen. *Brain Res.* **494**, 65–74 (1989).
- Uosaki, H. *et al.* Efficient and scalable purification of cardiomyocytes from human embryonic and induced pluripotent stem cells by VCAM1 surface expression. *PLoS One* **6**, e23657 (2011).
- Carpenter, L. *et al.* Efficient differentiation of human induced pluripotent stem cells generates cardiac cells that provide protection following myocardial infarction in the rat. *Stem Cells Dev.* **21**, 977–986 (2012).
- Graichen, R. *et al.* Enhanced cardiomyogenesis of human embryonic stem cells by a small molecular inhibitor of p38 MAPK. *Differentiation* **76**, 357–370 (2008).
- Melkounian, Z. *et al.* Synthetic peptide-acrylate surfaces for long-term self-renewal and cardiomyocyte differentiation of human embryonic stem cells. *Nat. Biotechnol.* **28**, 606–610 (2010).
- Nagaoka, M., Si-Tayeb, K., Akaike, T. & Duncan, S.A. Culture of human pluripotent stem cells using completely defined conditions on a recombinant E-cadherin substratum. *BMC Dev. Biol.* **10**, 60 (2010).
- Braam, S.R. *et al.* Recombinant vitronectin is a functionally defined substrate that supports human embryonic stem cell self-renewal via alphavbeta5 integrin. *Stem Cells* **26**, 2257–2265 (2008).
- Rodin, S. *et al.* Clonal culturing of human embryonic stem cells on laminin-521/E-cadherin matrix in defined and xeno-free environment. *Nat. Commun.* **5**, 3195 (2014).
- Rodin, S. *et al.* Long-term self-renewal of human pluripotent stem cells on human recombinant laminin-511. *Nat. Biotechnol.* **28**, 611–615 (2010).
- Miyazaki, T. *et al.* Laminin E8 fragments support efficient adhesion and expansion of dissociated human pluripotent stem cells. *Nat. Commun.* **3**, 1236 (2012).
- Domogatskaya, A., Rodin, S. & Tryggvason, K. Functional diversity of laminins. *Annu. Rev. Cell Dev. Biol.* **28**, 523–553 (2012).
- Tohyama, S. *et al.* Distinct metabolic flow enables large-scale purification of mouse and human pluripotent stem cell-derived cardiomyocytes. *Cell Stem Cell* **12**, 127–137 (2013).
- Paige, S.L. *et al.* Endogenous Wnt/beta-catenin signaling is required for cardiac differentiation in human embryonic stem cells. *PLoS One* **5**, e11134 (2010).
- Martin, A.F. Turnover of cardiac troponin subunits. Kinetic evidence for a precursor pool of troponin-I. *J. Biol. Chem.* **256**, 964–968 (1981).
- Ng, S.Y., Wong, C.K. & Tsang, S.Y. Differential gene expressions in atrial and ventricular myocytes: insights into the road of applying embryonic stem cell-derived cardiomyocytes for future therapies. *Am. J. Physiol. Cell Physiol.* **299**, C1234–C1249 (2010).
- Minami, I. *et al.* A small molecule that promotes cardiac differentiation of human pluripotent stem cells under defined, cytokine- and xeno-free conditions. *Cell Reports* **2**, 1448–1460 (2012).
- Chuva de Sousa Lopes, S.M. *et al.* Patterning the heart, a template for human cardiomyocyte development. *Dev. Dyn.* **235**, 1994–2002 (2006).
- Bird, S.D. *et al.* The human adult cardiomyocyte phenotype. *Cardiovasc. Res.* **58**, 423–434 (2003).
- Xie, C., Lin, Z., Hanson, L., Cui, Y. & Cui, B. Intracellular recording of action potentials by nanopillar electroporation. *Nat. Nanotechnol.* **7**, 185–190 (2012).
- Francis, G.L. Albumin and mammalian cell culture: implications for biotechnology applications. *Cytotechnology* **62**, 1–16 (2010).
- Takahashi, T. *et al.* Ascorbic acid enhances differentiation of embryonic stem cells into cardiac myocytes. *Circulation* **107**, 1912–1916 (2003).
- Cao, N. *et al.* Ascorbic acid enhances the cardiac differentiation of induced pluripotent stem cells through promoting the proliferation of cardiac progenitor cells. *Cell Res.* **22**, 219–236 (2012).
- Blaschke, K. *et al.* Vitamin C induces Tet-dependent DNA demethylation and a blastocyst-like state in ES cells. *Nature* **500**, 222–226 (2013).
- Moyes, K.W. *et al.* Human embryonic stem cell-derived cardiomyocytes migrate in response to gradients of fibronectin and Wnt5a. *Stem Cells Dev.* **22**, 2315–2325 (2013).
- Tribulova, N. *et al.* Enhanced connexin-43 and alpha-sarcomeric actin expression in cultured heart myocytes exposed to triiodo-L-thyronine. *J. Mol. Histol.* **35**, 463–470 (2004).
- Wang, B., Ouyang, J. & Xia, Z. Effects of triiodo-thyronine on angiotensin-induced cardiomyocyte hypertrophy: reversal of increased beta-myosin heavy chain gene expression. *Can. J. Physiol. Pharmacol.* **84**, 935–941 (2006).
- Zhang, Q. *et al.* Direct differentiation of atrial and ventricular myocytes from human embryonic stem cells by alternating retinoid signals. *Cell Res.* **21**, 579–587 (2011).

ONLINE METHODS

Cultures. All pluripotent and reprogramming cultures were maintained at 37 °C in a New Brunswick Galaxy 170R humidified incubator (Eppendorf), with 5% CO₂ and 5% O₂ controlled by the injection of carbon dioxide and nitrogen. Primary cell and differentiation cultures were maintained at 5% CO₂ and atmospheric (21%) O₂.

Human induced pluripotent cell derivation. Protocols were approved by the Stanford University Human Subjects Research Institutional Review Board. With informed written consent, two 2-mm skin punch biopsies were taken from each volunteer, diced with a scalpel, digested with 1 mg/ml collagenase IV (Life Technologies) for 2 h at 37 °C. Fibroblasts were then grown in DMEM with GlutaMAX (Life Technologies) supplemented with 10% FBS (US origin, Life Technologies) on six-well plates (Greiner) coated with a 1:200 dilution of growth factor–reduced Matrigel (9 µg/cm², Corning). Medium was changed every other day. When confluent, fibroblasts were passaged with TrypLE Express (Life Technologies) onto Matrigel-coated T225 flasks (Nunc).

For Sendai virus-based reprogramming (**Supplementary Fig. 1a**), early passage (passage 2 to passage 3) fibroblasts were seeded at 40,000 cells per well on Synthemax II-SC¹⁸ (625 ng/cm², Corning)-coated six-well plates. After 24 h, medium was changed to E8 medium⁴¹. The E8 formula was modified to replace human-derived transferrin with an *Oryza sativa*–derived recombinant version, to make the formula completely chemically defined. The successful application of Synthemax II-SC at the low concentration of 625 ng/cm² is in line with reports⁴² that the minimal surface density of vitronectin protein is very low at 250 ng/cm². E8 medium consisting of DMEM-F12 (50:50 mixture of DMEM and Ham's F12 medium; 10-092-CM, Corning), 20 µg/ml *Escherichia coli*–derived recombinant human insulin (Dance Pharmaceuticals/CS Bio), 64 µg/ml L-ascorbic acid 2-phosphate sesquimagnesium salt hydrate (Sigma-Aldrich), 10.7 µg/ml *O. sativa*–derived recombinant human transferrin (Optiferrin, Invitria/Sigma-Aldrich), 14 ng/ml sodium selenite (Sigma-Aldrich), 100 ng/ml recombinant human FGF2 (154 amino acid, *E. coli*–derived, Peprotech) and 2 ng/ml recombinant human TGFβ1 (112 amino acid, HEK293-derived, Peprotech). To the medium we added four OSKM CytoTune-iPS Sendai Reprogramming Kit viral particle factors (Life Technologies)⁴³ diluted ~1/5 on the basis of the manufacturer's recommendations (3 × 10⁵ cell infectious units (CIU) of each particle per well, multiplicity of infection (MOI) = 7.5). Medium was changed after 24 h and thereafter once every day. For the first 7 d, cultures were maintained in E8 medium supplemented with 100 nM hydrocortisone (Sigma-Aldrich) and 200 µM sodium butyrate (Sigma-Aldrich)⁴⁴. At day 7, medium was swapped to E7N (E8 minus TGFβ1; supplemented with 200 µM sodium butyrate). Medium switched to E8 medium at day 20.

For plasmid-based reprogramming⁴⁵, pCXLE-hSK (27078), pCXLE-hUL (27080) and pCXLE-hOCT4-shp53 (27077) plasmids were obtained from Addgene. The OSKM codon-optimized mini-intronic plasmid (CoMiP) was generated. Plasmid-containing *E. coli* were grown in Miller's LB (Life Technologies), and purified using Plasmid Maxi Kit (QIAGEN) following manufacturer's instructions, and quantified using a NanoDrop 2000 (Thermo

Scientific). 1 × 10⁶ cells were electroporated with 6 µg total DNA (2 µg of each for three plasmid-based systems, 6 µg for CoMiP) using a Neon Transfection System (Life Technologies), with the settings: 1,650 V, 3 pulses, 10 ms, 100 µl tips, and buffers R and E2. Cells were plated on Synthemax II-SC–coated six-well plates.

For peripheral blood mononuclear cell (PBMC) reprogramming, 20 ml of blood was collected in EDTA-containing Vacutainer tubes (BD Biosciences). PBMCs were isolated using a Ficoll-Paque PLUS (1.077 g/ml) gradient (GE Healthcare) and plated at 1 million cells per milliliter in 2 ml of a humanized version of blood medium⁴⁶ comprised of 50:50 IMDM:F12 (both Life Technologies), 2 mg/ml recombinant human albumin, 1% v/v chemically defined lipid concentrate (Life Technologies), 10 µg/ml recombinant human insulin, 100 µg/ml recombinant human transferrin, 15 ng/ml sodium selenite, 64 µg/ml L-ascorbic acid 2-phosphate, 450 µM 1-thioglycerol (Sigma-Aldrich), 50 ng/ml SCF (Peprotech), 10 ng/ml IL3 (Peprotech), 2 U/ml EPO (EMD Millipore), 40 ng/ml IGF1 (Peprotech) and 1 µM dexamethasone (Sigma-Aldrich). Cells were cultured for 9 d with 50% medium changes every other day. After 9 d, 1 × 10⁶ were plated in blood medium with Sendai virus, as above. Medium was changed every other day and were transferred to E7N medium in a Synthemax II-SC–coated six-well plate at day 3.

For all reprogramming methods, individual colonies with hESC morphology were picked into one well of a 12-well plate (one colony per well) at day 17 to day 25 in E8 medium with 2 µM thiazovivin for 24 h after picking. Subsequently, cells were expanded into six-well plates by passaging 1:1, 1:4, 1:6, 1:8 and finally 1:12, using 0.5 mM EDTA (Life Technologies) in D-PBS without CaCl₂ or MgCl₂ (Life Technologies) for 7 min at room temperature.

Human pluripotent stem cell culture. Cells were routinely maintained in E8 medium (made as above) on either Synthemax II-SC (625 ng/cm²) or 1:200 growth factor–reduced Matrigel (9 µg/cm²) and passaged every 4 d using 0.5 mM EDTA (as above). 2 µM thiazovivin (Selleck Chemicals) was added for the first 24 h after passage. Control hESC lines H7 (WA07) and H9 (WA09)⁴⁷ were supplied by WiCell Research Institute. All hESC and hiPSC lines were converted to E8 medium with EDTA–based culture for at least five passages before beginning differentiation. For the growth comparison experiment, cells were grown in mTeSR1 (Stemcell Technologies). Cell lines were used between passages 20 and 83. All cultures (primary, pluripotent and differentiation) were maintained with 2 ml medium per 9.6 cm² of surface area or equivalent. All pluripotent cultures were routinely tested for mycoplasma contamination using a MycoAlert Kit (Lonza).

Growth assays. To assess cell growth, cells were counted using a Countess automated cell counter (Life Technologies). For growth rate calculation, cells were seeded at 1.25 × 10⁴ cells per cm² (120,000 cells per well of a 6-well plate) and grown for 96 h. Cumulative population doublings was calculated using the formula $n = 3.32 (\log_{10}(N/N_0))$, where n is the number of population doublings, N is number of cells at passage, and N_0 is number of cells seeded).

Teratoma analysis. Three confluent wells of pluripotent cells were dissociated with EDTA, centrifuged, resuspended in 100 µl of growth factor–reduced Matrigel, and injected into the kidney

capsule of female 12–24 week-old nonobese diabetic severe combined immunodeficiency mice (NOD.CB17-*Prkdc*^{scid}/NcrCrl strain code 394, Charles River). After 4–6 weeks, teratomas were removed, fixed in 4% PFA, embedded in paraffin wax, sectioned and hematoxylin and eosin (H&E) stained by members of the Stanford Tissue Bank. Slides were imaged and analyzed by a qualified clinical pathologist. Animal studies were approved by Stanford Institution Review Board and Stem Cell Research Oversight committees.

Single nucleotide polymorphism karyotyping. A single well of greater than passage 20 (>p20) pluripotent cells was dissociated with 0.5 mM EDTA, pelleted and snap-frozen in liquid nitrogen. Genomic DNA was extracted using a Blood and Tissue DNA extraction kit (QIAGEN), following the manufacturer's directions. SNP karyotyping was performed using a Genome-Wide CytoScan HD Array (Affymetrix) covering 2.7 million markers and 750,000 SNPs, and was analyzed using Chromosome Analysis Suite (ChAS, Affymetrix).

Cardiac differentiation of hiPSCs. Both hiPSCs and hESCs (>p20) were split at 1:10 or 1:12 ratios, using EDTA as above and grown for 4 d, at which time they reached ~85% confluence. Medium was changed to CDM3, consisting of RPMI 1640 medium (11875, Life Technologies), 500 µg/ml *O. sativa*-derived recombinant human albumin (A0237, Sigma-Aldrich, 75 mg/ml stock solution in water for injection (WFI) quality H₂O, stored at –20 °C), and 213 µg/ml L-ascorbic acid 2-phosphate (Sigma-Aldrich, 64 mg/ml stock solution in WFI H₂O, stored at –20 °C). Medium was changed every other day (48 h). For day 0 to day 2, medium was supplemented with 6 µM CHIR99021 (LC Laboratories). On day 2, medium was changed to CDM3 supplemented with 2 µM Wnt-C59 (Selleck Chemicals). Medium was changed on day 4 and every other day for CDM3. Contracting cells were noted from day 7.

Other additions to cardiac differentiation medium tested were 10.7 µg/ml recombinant human transferrin, 14 µg/ml sodium selenite, 1 µg/ml linoleic acid, 1 µg/ml linolenic acid, 2 ng/ml triiodo-L-thyronine, 2 µg/ml L-carnitine, 1 µg/ml D,L-α-tocopherol acetate, 100 ng/ml retinol acetate, 1 µg/ml ethanolamine, 20 ng/ml corticosterone, 9 ng/ml progesterone, 47 ng/ml lipoic acid, 100 ng/ml retinol, 1 µg/ml D,L-α-tocopherol, 100 ng/ml biotin, 2.5 µg/ml catalase, 2.5 µg/ml glutathione, 2.5 µg/ml superoxide dismutase, 2 µg/ml L-carnitine, 15 µg/ml D(+)-galactose, 16.1 µg/ml putrescine, 450 µM L-thioglycerol, 55 µM 2-mercaptoethanol and 64 µg/ml L-ascorbic acid 2-phosphate (all from Sigma-Aldrich).

Basal media assessed were DMEM (11965), DMEM/F12 (11330), IMDM (12440), IMDM/F12 (12440/11765), RPMI 1640 medium (11875), McCoy's 5A (16600), M199 (with Earle's salts, 11150), MEMα (with Earle's salts, no nucleosides, 12561) and MEM (with Earle's salts, 11095) (all from Life Technologies). RPMI 1640 media assessed were RPMI 1640 with L-glutamine (11875), RPMI 1640 with L-glutamine and HEPES (22400), RPMI 1640 with GlutaMAX (61870) and RPMI with GlutaMAX and HEPES (72400) (all from Life Technologies).

Albumin sources assessed were human serum albumin (A1653, Sigma-Aldrich), *O. sativa*-derived recombinant human albumin (A0237, Sigma-Aldrich), *Saccharomyces cerevisiae*-derived recombinant Albucult (Novozymes Biopharma/A6608, Sigma Aldrich),

O. sativa-derived recombinant Cellastim (Invitria/A9731, Sigma Aldrich) and embryo-grade BSA (A3311, Sigma Aldrich).

Wnt inhibitors assessed were IWP-2, IWR-1 (both Sigma-Aldrich), XAV-939, ICG-001 (Selleck Chemicals), IWP-4 (Stemgent) and Wnt-C59 (Selleck Chemicals). GSK3B inhibitors assessed were CHIR99021 (LC Laboratories), BIO, TWS119 (Selleck Chemicals), 1-azekapallone, TDZD-8, ARA014418 and 3F8 (all Sigma-Aldrich). Inhibitors used for pathway analysis were PD173074, SB203580, LDN193189, SB431542 (all Selleck Chemicals), SU5402, dorsomorphin, A83-01 (all Tocris), ALK5 inhibitor (Stemgent) and ITD-1 (Xcessbio). All small molecules were resuspended to 10 mM in dimethyl sulfoxide (DMSO) and used at 5 µM except for Wnt-C59, which was used at 2 µM.

For control treatments (0 µM) 0.1% DMSO was used. Comparisons of differentiation media were made to RPMI + B27 – ins medium consisting of RPMI 1640 medium (11875) supplemented with 2% B27 without insulin (0050129SA, Life Technologies) and StemPro-34 medium (Life Technologies) supplemented as shown in **Supplementary Table 1**. LI-APEL low-insulin medium and 'xeno-free' differentiation medium were made as described^{2,9,48}. For optimization of cardiac differentiation conditions, cells were differentiated in 12-well plates, and samples were analyzed at day 15 of differentiation after dissociation with TrypLE Express for 10 min at 37 °C.

Matrices. The following matrices were assessed for the ability to support pluripotent growth and subsequent cardiac differentiation: 9 µg/cm² growth-factor reduced Matrigel (1:200, Corning) in DMEM/F12; 625 ng/cm² vitronectin peptide (Synthemax II-SC, 1:320, Corning) in ultrapure water (1:50 dilution was also tested); 1 µg/cm² full length recombinant human vitronectin (1:50, Primorigen) in D-PBS with CaCl₂ and MgCl₂; 2.5 µg/cm² laminin-521 (1:80, Biolamina) in DPBS; 2 µg/cm² truncated recombinant human laminin-511 iMatrix-511 (1:50, Iwai North America) in DPBS; 1 µg/cm² recombinant human E-cadherin (1:25, StemAdhere, Primorigen/Stemcell Technologies); and 10 µg/cm² fibronectin (1:20, EMD Millipore) in D-PBS. All were used at 2 ml per well of a six-well plate (9.6 cm²). Matrices were assessed on both six-well polystyrene tissue culture plates and untreated plates (both from Greiner). Also tested were Synthemax-T six-well plates, and fibronectin mimetic plates (both from Corning) and 10 µg/cm² Pronectin (Sigma-Aldrich).

In vitro purification of cardiomyocytes. To purify cardiomyocytes, a variant of RPMI 1640 medium without D-glucose (11879, Life Technologies) was used in the medium formula. RPMI medium without D-glucose was supplemented with 213 µg/ml L-ascorbic acid 2-phosphate (Sigma-Aldrich), 500 µg/ml *O. sativa*-derived recombinant human albumin (Sigma-Aldrich) and 5 mM sodium DL-lactate (L4263, Sigma-Aldrich), and used in place of CDM3 on differentiation days 10–20.

Cryopreservation of purified cardiomyocytes. Differentiation day 15 cardiomyocytes were treated with TrypLE for 10 min at 37 °C and triturated with a P1000 tip. Cells were filtered through a 100 µm cell strainer (Corning), counted using a Countess Cell Counter (Life Technologies) and cryopreserved at 2–50 million cells per vial in CDM3 + 10% DMSO using a BioCision CoolCell.

Immunofluorescence staining. hiPSCs or cardiomyocytes were plated onto Synthemax II-SC-coated Lab-Tek II eight-chamber glass slides (154524, Nunc) and were allowed to grow for 3 d. Cells were fixed with 4% PFA (Electron Microscopy Services) for 15 min at room temperature, permeabilized with 0.1% Triton-X (Sigma-Aldrich) for 10 min at room temperature, blocked in 10% goat serum (Sigma-Aldrich) and 0.1% Triton-X for 15 min at room temperature, and stained with 1:200 mouse IgM TRA-1-60 (09-0010), 1:200 mouse IgM_k TRA-1-80 (09-0012), 1:200 mouse IgG₃ SSEA4 (09-0006, all Stemgent), 1:200 rabbit IgG POU5F1 (sc-9081), 1:200 rabbit IgG NANOG (sc-33759, both Santa Cruz Biotechnology), 1:200 rabbit IgG SOX2 (651901, Biolegend), 1:200 mouse monoclonal IgG₁ TNNT2 (13-11, Thermo Scientific), 1:200 rabbit monoclonal IgG α -actinin (H-300, Santa Cruz), 1:400 mouse monoclonal IgG_{2b} MLC2A (MYL7, Synaptic Systems), 1:200 rabbit polyclonal IgG MLC2V (MYL2, ProteinTech), 1:50 mouse monoclonal IgG₁ P4HB (Abcam), 1:400 mouse monoclonal IgG_{2a} SMA (Sigma-Aldrich), 1:400 rabbit polyclonal IgG vWF (Abcam) or 1:500 rabbit polyclonal IgG Ki67 (Thermo Scientific) overnight at 4 °C in 1% BSA in D-PBS. Cells were washed four times, for 10 min, with 1% BSA in D-PBS-T and then incubated for 1 h at room temperature in the dark with secondary antibodies 1:1,000 Alexa Fluor 488 goat anti-mouse IgM (μ chain), 1:1,000 Alexa Fluor 488 goat anti-mouse IgG (H+L) or 1:1,000 Alexa Fluor 594 goat anti-rabbit IgG (H+L) (all Life Technologies) in 1% BSA in D-PBS. Cells were washed again as above, nuclei were stained with NucBlue Fixed Cell Stain (Life Technologies), and coverslips were attached to Superfrost Plus (Thermo Scientific) slides with Vectashield (Vectorlabs) and imaged with an LSM510Meta Confocal Microscope (Zeiss).

Flow cytometry. Cells were transferred to flow cytometry tubes (BD Biosciences) and fixed with 1% PFA for 15 min, permeabilized with 90% methanol for 15 min, and stained using 1:200 rabbit polyclonal IgG POU5F1 (H-134, sc-9081, Santa Cruz Biotechnology), 1:20 mouse monoclonal IgG₃ SSEA4-APC (clone MC-813-70, FAB1435A, R&D Systems), 1:200 NANOG rabbit polyclonal IgG (H-155, sc-33759, Santa Cruz Biotechnology), 1:20 mouse monoclonal IgM TRA-1-60-FITC (FAB4770P, R&D Systems), 1:200 mouse monoclonal IgG₁ TNNT2 (cardiac troponin T, 13-11, MS-295-P, Thermo Scientific), 1:200 mouse monoclonal IgG₁ TNNT2 (cardiac troponin T, clone 1C11, ab8295, Abcam), 1:200 mouse monoclonal IgG_{2b} TNNT2 (cardiac and skeletal troponin I, clone 2Q1100, T8665-16M, US Biological), 1:400 mouse monoclonal IgG_{2b} MLC2A (MYL7, Synaptic Systems) and 1:200 rabbit polyclonal IgG MLC2V (MYL2, ProteinTech) for 45 min at room temperature. Isotype controls used were mouse IgG₁ (557273, BD Biosciences), mouse IgG_{2b} (16-4724-82, eBiosciences) and rabbit IgG (02-6102, Life Technologies). Secondary staining was performed with 1:1,000 Alexa Fluor 488 goat anti-mouse IgG₁, 1:1,000 Alexa Fluor 488 goat anti-rabbit IgG (H+L), 1:1,000 Alexa Fluor 647 goat anti-mouse IgG_{2b} and 1:1,000 Alexa Fluor 647 goat anti-rabbit IgG (H+L) secondary antibodies (all Life Technologies) for 20 min. These conditions were shown to stain negative on human skin fibroblasts. Cells were analyzed using a FACSAria II (BD Biosciences) with a 100 μ m nozzle and FACSDiva software. Data were analyzed using FlowJo 8.7 (TreeStar).

For optimization of cardiac troponin T (TNNT2) flow cytometry staining, we stained fibroblasts (45 min, primary) with the TNNT2 antibody 13-11 and observed a very minor increase in staining over the isotype control (**Supplementary Fig. 3g**). We also assessed additional monoclonal antibodies for cardiac troponin T (1-C11) and cardiac troponin I (7E147), each from a different manufacturer, and found similar levels of positive cell detection (~85–88%) (**Supplementary Fig. 3g**). As part of our optimization we also assessed overnight primary antibody staining with the TNNT2 13-11 antibody and found that this method gave us nonspecific staining in fibroblasts and raised the percentage of TNNT2⁺ cells to >99%. Therefore we used 45 min staining as above (**Supplementary Fig. 3g**).

Quantitative real-time PCR. To analyze gene expression, cells were dissociated with TryPLE Express, and pellets of cells were snap-frozen in liquid nitrogen and stored at –80 °C. RNA was isolated using an RNeasy Plus kit (QIAGEN), cDNA was produced using a High Capacity RNA-to-cDNA kit (Life Technologies), and real-time PCR was performed using TaqMan Gene Expression Assays (**Supplementary Table 5**), TaqMan Gene Expression Master Mix, and a 7900HT Real-Time PCR System (all Life Technologies). All PCR reactions were performed in triplicate, normalized to the 18S endogenous control gene, and assessed using the comparative change in threshold cycle (ΔC_t) method.

Single-cell quantitative real-time PCR. To analyze single-cell gene expression, cells were dissociated as above, and a 300,000 cells/ml suspension was prepared. The cell suspension was loaded onto a 17–25 μ m C₁ Fluidigm chip for single-cell capture and treated with a LIVE/DEAD Viability/Cytotoxicity Kit (Life Technologies). The C₁ chip was then imaged under phase-contrast and fluorescence microscopes to exclude doublets and dead cells from subsequent PCR analysis. Single-cell lysis, reverse transcription and preamplification were all performed on the C₁ chip using the C₁ Single Cell Auto Prep (Fluidigm) and Single Cell-to-CT kits (Ambion). Reverse transcription was performed at 25 °C for 10 min, 42 °C for 1 h, and finally 85 °C for 5 min. Preamplification was performed at 95 °C for 10 min, followed by 18 cycles of 95 °C for 15 s, and 60 °C for 4 min. Amplified cDNA products were harvested from the C₁ chip into 96-well 0.2 ml PCR plates and then loaded onto Biomark 48.48 Dynamic Array chips using the Nanoflex IFC controller (Fluidigm). Quantitative single-cell PCR was performed using gene amplification with TaqMan Assays (Life Technologies) (**Supplementary Table 6**), and C_t as a measurement of relative fluorescence intensity was extracted by the BioMark Real-Time PCR Analysis software. All PCR reactions were performed in duplicate or triplicate, and C_t values were directly used in data analysis after normalization to the 18S endogenous control gene.

Patch clamp. To record cellular action potentials, cardiomyocytes at day 15 were dissociated using TryPLE for 10 min, filtered through a 100 μ m cell strainer (BD Biosciences), counted with a Countess Cell Counter, plated as single cells (1×10^5 cells per well of a 24-well plate) on 8 mm no. 1 glass cover slips (Warner Instruments) coated with Synthemax II-SC (625 ng/cm²) in CDM3 supplemented with 2 μ M thiazovivin and allowed to attach for 72 h, changing the medium every other day. Cells were then

subjected to whole-cell patch clamp at 36–37 °C, using an EPC-10 patch-clamp amplifier (HEKA) attached to a RC-26C recording chamber (Warner Instruments) and mounted onto the stage of an inverted microscope (Nikon). Sharp microelectrodes were fabricated from standard wall borosilicate glass capillary tubes (BF 100-50-10, Sutter Instruments) using a P-97 Sutter micropipette puller to generate electrodes with tip resistances between 50 M Ω and 70 M Ω when backfilled with 3 M KCl. Cell cultures were perfused with warm (35–37 °C) Tyrode's solution consisting of 135 mM NaCl, 5.4 mM KCl, 1.8 mM CaCl₂, 1.0 mM MgCl₂, 0.33 mM NaH₂PO₄, 5 mM HEPES and 5 mM glucose; pH was adjusted to 7.4 with NaOH. Membrane potential measurements were made using the current clamp mode of the Multiclamp 700B amplifier after electrode potential offset and capacitance were neutralized. Data were acquired using PatchMaster software (HEKA) and digitized at 1.0 kHz. The following are the criteria used for classifying observed action potentials (APs) into ventricular-, atrial- and Nodal-like hiPSC-derived cardiomyocytes. For ventricular-like, the criteria were a negative maximum diastolic membrane potential (<–50 mV), a rapid AP upstroke, a long plateau phase, AP amplitude > 90 mV and AP duration at 90% repolarization/AP duration at 50% repolarization (APD)₉₀/APD₅₀ < 1.4. For atrial-like, the criteria were an absence of a prominent plateau phase, a negative diastolic membrane potential (<–50 mV) and APD₉₀/APD₅₀ > 1.7. For Nodal-like, the criteria were a more positive MDP, a slower AP upstroke, a prominent phase 4 depolarization and APD₉₀/APD₅₀ between 1.4 and 1.7.

Nanopillar action potential recordings. Before plating, nanopillar electrode devices³² were cleaned with 5 min of oxygen plasma treatment. The culture chamber was coated with 9 μ g/cm² Matrigel for 30–60 min. hiPSC CMs were then plated at a density of 1×10^5 per cm in CDM3 with 2 μ M thiazovivin for the first 24 h. The cells were maintained in a standard incubator at 37 °C and 5% CO₂. Medium was changed every 24 h. 2–3 d after plating, spontaneous and synchronous beating was observed. A 60-channel voltage amplifier system (Multichannel System, MEA1060-Inv-BC) was used for recording hiPSC-derived cardiomyocytes cultured on nanopillar electrode arrays (9 nanopillars per array) after cells started beating. Recording was performed in the same culture medium at room temperature, using an Ag-AgCl electrode in the medium as the reference electrode. The amplification was 53

and the sampling rate was 5 kHz. For electroporation, 20 biphasic square pulses of 3.5 V amplitude and 400 μ s period were applied to a nanopillar electrode. The recording system was blanked during the electroporation period. Electrophysiology recordings were resumed 10–20 s after the electroporation to avoid amplifier saturation. Recordings were taken daily. The recordings were analyzed by a custom Matlab (Mathworks) code. Briefly, the first 20–30 intracellular recorded action potentials were overlaid and averaged. The action potential maximum and resting potentials were then identified. APD₅₀ and APD₉₀ were subsequently computed. Similar to multielectrode array recordings, nanopillar intracellular recordings register a signal amplitude of 1–2 mV. This is because the seal resistance between the cell and the nanoelectrodes does not rely on achieving a gigaohm seal. However, we have demonstrated that the signal morphologies recorded by the nanopillar are identical to those recorded by patch clamp electrophysiology⁴⁹. Nanopillar electrode devices were reused after removal of the cells by TrypLE Express.

41. Chen, G. *et al.* Chemically defined conditions for human iPSC derivation and culture. *Nat. Methods* **8**, 424–429 (2011).
42. Yap, L.Y. *et al.* Defining a threshold surface density of vitronectin for the stable expansion of human embryonic stem cells. *Tissue Eng. Part C Methods* **17**, 193–207 (2011).
43. Fusaki, N., Ban, H., Nishiyama, A., Saeki, K. & Hasegawa, M. Efficient induction of transgene-free human pluripotent stem cells using a vector based on Sendai virus, an RNA virus that does not integrate into the host genome. *Proc. Jpn. Acad., Ser. B, Phys. Biol. Sci.* **85**, 348–362 (2009).
44. Mali, P. *et al.* Butyrate greatly enhances derivation of human induced pluripotent stem cells by promoting epigenetic remodeling and the expression of pluripotency-associated genes. *Stem Cells* **28**, 713–720 (2010).
45. Okita, K. *et al.* A more efficient method to generate integration-free human iPS cells. *Nat. Methods* **8**, 409–412 (2011).
46. Chou, B.K. *et al.* Efficient human iPS cell derivation by a non-integrating plasmid from blood cells with unique epigenetic and gene expression signatures. *Cell Res.* **21**, 518–529 (2011).
47. Thomson, J.A. *et al.* Embryonic stem cell lines derived from human blastocysts. *Science* **282**, 1145–1147 (1998).
48. Ng, E.S., Davis, R., Stanley, E.G. & Elefanty, A.G. A protocol describing the use of a recombinant protein-based, animal product-free medium (APEL) for human embryonic stem cell differentiation as spin embryoid bodies. *Nat. Protoc.* **3**, 768–776 (2008).
49. Lin, Z.C., Xie, C., Osakada, Y., Cui, Y. & Cui, B. Iridium oxide nanotube electrodes for sensitive and prolonged intracellular measurement of action potentials. *Nat. Commun.* **5**, 3206 (2014).